

Published in final edited form as:

*Biochem Biophys Res Commun.* 2011 August 19; 412(1): 55–60. doi:10.1016/j.bbrc.2011.07.036.

## Are Mitochondrial Reactive Oxygen Species Required for Autophagy?

Jianfei Jiang<sup>a,\*</sup>, Akihiro Maeda<sup>a,1</sup>, Jing Ji<sup>a</sup>, Catherine J. Baty<sup>b</sup>, Simon C. Watkins<sup>b</sup>, Joel S. Greenberger<sup>c</sup>, and Valerian E. Kagan<sup>a,\*</sup>

<sup>a</sup>Center for Free Radical and Antioxidant Health, Department of Environmental and Occupational Health, University of Pittsburgh

<sup>b</sup>Center for Biologic Imaging, Department of Cell Biology and Physiology, University of Pittsburgh

<sup>c</sup>Department of Radiation Oncology, University of Pittsburgh

### Abstract

Reactive oxygen species (ROS) are said to participate in the autophagy signaling. Supporting evidence is obscured by interference of autophagy and apoptosis, whereby the latter heavily relies on ROS signaling. To dissect autophagy from apoptosis we knocked down expression of cytochrome c, the key component of mitochondria-dependent apoptosis, in HeLa cells using shRNA. In cytochrome c deficient HeLa1.2 cells, electron transport was compromised due to the lack of electron shuttle between mitochondrial respiratory complexes III and IV. A rapid and robust LC3-I/II conversion and mitochondria degradation were observed in HeLa1.2 cells treated with staurosporine (STS). Neither generation of superoxide nor accumulation of H<sub>2</sub>O<sub>2</sub> was detected in STS-treated HeLa1.2 cells. A membrane permeable antioxidant, PEG-SOD, plus catalase exerted no effect on STS-induced LC3-I/II conversion and mitochondria degradation. Further, STS caused autophagy in mitochondria DNA-deficient ρ<sup>0</sup> HeLa1.2 cells in which both electron transport and ROS generation were completely disrupted. Counter to the widespread view, we conclude that mitochondrial ROS are not required for the induction of autophagy.

### Keywords

apoptosis; autophagy; reactive oxygen species; cytochrome c deficient; HeLa cells; staurosporine

## 1. Introduction

Reactive oxygen species (ROS) are known signaling molecules in a variety of intracellular pathways, leading to proliferation, apoptosis, immunity and defense against microorganisms. Recently, ROS have been implicated in the signaling of autophagy [1–3] - an evolutionarily conserved degradation pathway which functions as a cell survival adaptive mechanism during stress conditions [4–6]. Autophagy can be triggered by a variety of intracellular and extracellular stimuli, including those that cause damage to organelles, starvation, protein

© 2011 Elsevier Inc. All rights reserved.

\*Corresponding author. Address: 100 Technology Drive, Bridgeside Point, Suite 350, Pittsburgh, PA, 15219 USA. Tel: 412-624-9479, Fax: 412-624-9361, kagan@pitt.edu (V.E. Kagan), jjf73@pitt.edu (J. Jiang).

<sup>1</sup>These two authors contribute equally to this work.

**Publisher's Disclaimer:** This is a PDF file of an unedited manuscript that has been accepted for publication. As a service to our customers we are providing this early version of the manuscript. The manuscript will undergo copyediting, typesetting, and review of the resulting proof before it is published in its final citable form. Please note that during the production process errors may be discovered which could affect the content, and all legal disclaimers that apply to the journal pertain.

aggregation, and pathogen infection. The exact molecular mechanisms by which these stimuli provoke autophagy, however, remain largely elusive. A growing body of studies has suggested a signaling role of mitochondrial ROS in autophagy. Kirkland *et al* [1] demonstrated that NGF-deprived sympathetic neurons produced mitochondrial ROS that caused lipid peroxidation and loss of cardiolipin (CL), resulting in autophagic cell death. ROS were suggested to be both sufficient and essential for tumor necrosis factor- $\alpha$  induced autophagy [2]. Chen *et al* demonstrated that mitochondrial electron transport chain (*mtETC*) inhibitors of complexes I and II, such as rotenone and thenoyltrifluoroacetone, induced autophagy mediated by ROS [3].

Although a number of studies have established a temporal association between mitochondrial ROS and autophagy, it remains to be understood whether induction of autophagy is a part of the repair response to damage caused by ROS or ROS are directly implicated in the execution mechanisms of autophagy [7]. The difficulties in addressing the dilemma are due to the fact that experimental manipulations of ROS generation often affect apoptosis [8,9] whose execution mechanisms – in cases of intrinsic apoptosis and type II extrinsic apoptosis - heavily rely on mitochondrial ROS production. In particular, collapse of mitochondrial CL asymmetry and its migration from the inner to the outer membrane, occurring early in apoptosis, facilitate the formation of cytochrome *c* (cyt *c*)/CL complex [10]. The latter utilizes mitochondrial ROS to cause accumulation of CL peroxidation products that participate in membrane permeabilization leading to the release of apoptotic factors from mitochondria into the cytosol [10,11]. The complex relationships between the processes of apoptosis and autophagy may range from synergy to mutual suppression depending on specificity of stimuli and intracellular conditions [12,13]. A mixed phenotype of apoptosis and autophagy is frequently detected in response to many stimuli - including ROS - indicating that these processes may share common upstream pathways [8]. Therefore, understanding whether mitochondrial ROS are required for the activation of autophagy is difficult, if not impossible, without dissecting the apoptotic and autophageal signaling pathways.

In this report, we utilized cyt *c* deficient HeLa cells in which we induced autophagy by staurosporine (STS) independently of apoptosis [10,14]. The compromised *mtETC* in cyt *c* deficient cells - due to the lack of electron shuttling between complexes III and IV - provided additional advantage for exploring the relationships between mitochondrial ROS and autophagy. Importantly, generation of ROS could be manipulated without affecting the apoptosis signaling pathway in cyt *c* deficient cells. In addition, we examined autophagy in  $\rho^{\circ}$  HeLa1.2 cells with depleted mitochondrial DNA (*mtDNA*), hence disrupted electron transport and ROS generation. Our results indicate that mitochondrial ROS are not essential for autophagy signaling.

## 2. Materials and Methods

### 2.1. Materials

Annexin-V kit was from Biovision (Mountain View, CA, USA). Dihydroethidium (DHE), 2',7'-dichlorfluoresceine-diacetate (DCFH-DA), and STS were from Invitrogen (Carlsbad, CA, USA). Mouse anti-LC3 antibody was from Nanotools (Teningen, Germany). Mouse anti-cytochrome *c* oxidase subunit IV (COX-IV) antibody was from Abcam (Cambridge, MA, USA) and anti- $\beta$ -actin antibody was from Sigma (St. Louis, MO, USA). Vectors expressing fluorescent sensor HyPer are from Evrogen (Moscow, Russia). All other reagents were from Sigma unless otherwise specified.

## 2.2. Cell Culture

Cyt *c* deficient HeLa1.2 cells were generated using shRNA procedure and maintained in DMEM medium [11]. To develop *mtDNA* deficient  $\rho^0$  cells, HeLa1.2 cells were exposed to 50 ng/ml ethidium bromide for 60 days.

## 2.3. Phosphatidylserine (PS) externalization

Externalization of PS and cell membrane integrity were analyzed by flow cytometry (FACScanto II, BD, NJ, USA) using an Annexin-V/propidium iodide (PI) kit. Percentages of Annexin-V-positive cells were calculated by combining Annexin V+/PI- and Annexin V+/PI+ cells.

## 2.4. Western blotting

Cells were lysed in RIPA buffer containing protease inhibitors cocktail. The resulting supernatants after centrifugation (5,000g/5min/4°C) were subjected to 15% SDS-PAGE and then transferred to nitrocellulose membrane. The membrane was blocked with casein and probed with antibodies against LC3, COX-IV and  $\beta$ -actin (loading control) followed by horseradish peroxidase-coupled detection.

## 2.5. GFP-LC3 punctate

Cells were transiently transfected with pGFP-LC3 [15] (provided by Dr. Yoshimori, Japan) using Optifect transfection reagent (Invitrogen). The punctuate formation of GFP-LC3 proteins following STS-treatment was observed using an Olympus Fluoview 1000 confocal microscope (Olympus, Japan). Images shown are representatives of three independent experiments.

## 2.6. Transmission electron microscopy (TEM)

Cells grown in 6-well tissue culture dishes were rinsed with PBS, fixed in 2.5% glutaraldehyde overnight at 4°C, and processed for imaging on a JEOL JEM-1011 (JEOL, Tokyo, Japan) transmission electron microscope.

## 2.7. Superoxide generation

At the indicated time points, cells were incubated with 10  $\mu$ M DHE for 30 min. The mean ethidium fluorescence intensity from 10,000 cells was acquired by a FACScanto II flow cytometer using a 585/42 nm bandpass filter. The data are presented by fold change of the mean intensity of ethidium fluorescence compared with DHE loaded control cells.

## 2.8. Hydrogen peroxide assay

The intracellular hydrogen peroxide was evaluated using a genetically encoded fluorescent sensor-HyPer [16]. In brief, HeLa and HeLa1.2 cells were transfected with pHyPer using Optifect transfection reagent. After 48 post-transfection incubation, cells were treated with 100 nM STS (1–6 h). At the end of treatment, the green fluorescence (530/30 nm bandpass filter) in transfected cells after excitation at 488 and 405 nm was measured using a BD FACSAria II SORP flow cytometer. The production of intracellular  $H_2O_2$  was evaluated by calculating the ratio of green fluorescence excited at 488 and 405 nm. As positive control, transfected cells were treated with  $H_2O_2$  prior to flow analysis. In parallel, time-lapse images were recorded to monitor the oxidation of HyPer sensor using a Nikon Eclipse Ti microscope system (at 380/510 and 480/525 nm of excitation/emission wavelength) equipped with NIS-Elements software. Additionally, the intracellular hydrogen peroxide generation was determined using DCFH-DA. Briefly, cells were incubated with 10  $\mu$ M DCFH-DA for 30 min; at the indicated time points, the fluorescence of dichlorofluoresceine

(DCF, a DCFH oxidation product, 530/30 nm bandpass filter) was evaluated using FACScanto II flow cytometer.

## 2.9. Statistics

All data are expressed as means $\pm$ SD of at least three independent experiments. Statistical comparisons between groups were performed by Student's *t*-test.  $P < 0.05$  was considered significant.

## 3. Results

### 3.1. Dissection of autophagy and apoptosis in STS-treated cyt c deficient HeLa1.2 cells

A mixed phenotype of apoptosis and autophagy is characteristic of STS-induced injury in HeLa cells [17,18]. Although the exact mechanisms of STS action remain controversial, it is generally believed that mitochondria play a critical role in execution of apoptosis [19]. To dissect the pathways of apoptosis and autophagy, we employed a cyt *c* deficient HeLa cell line (HeLa1.2) [10] lacking this key component of mitochondrial apoptotic machinery. HeLa and HeLa1.2 cells were treated with STS (25–100 nM) for 18-h and apoptosis was evaluated by determining PS externalization using flow cytometry. STS caused a strong dose-dependent increase in the number of PS-positive HeLa cells that exceeded 50% at 100 nM STS. In contrast, the percentage of PS-positivity for cyt *c* deficient HeLa1.2 cells was low and remained below 10% even after exposure to 100 nM STS (Fig.1A).

We next examined the STS-induced autophagic flux in HeLa and HeLa1.2 cell by determining the conversion of LC3-I to autophagosome associated phosphatidylethanolamine (PE)-conjugated LC3-II form [15]. Exposure to 100 nM STS resulted in time-dependent decrease of LC3-I with concomitant accumulation of LC3-II as evidenced by Western blotting (Fig.2A). The STS-induced LC3-I/II conversion was blocked by wortmannin (WT, PI3-kinase inhibitor) and enhanced by bafilomycin A1 (BafA1, lysosomal inhibitor) (Fig.2B,C) thus providing further evidence for the autophageal changes in STS-treated cells. The occurrence of autophagy in HeLa1.2 cells was also confirmed (Fig. 2E–H) by utilizing GFP-LC3 [15]. Under normal conditions, the GFP-LC3 was diffusely distributed in the cytosol of HeLa1.2 cells. Upon STS treatment (100 nM, 3 and 6-h), LC3 exhibited a bright punctate pattern indicative of the formation of isolation membranes and autophagosomes. After treatment with 3 mM 3-methyladenine (3-MA, PI3-kinase inhibitor), the diffuse pattern of GFP-LC3 fluorescence remained unchanged in most cells. As an additional indicator of autophagic activity, the development of acidic vascular organelles (AVO) was examined with a vital Acridine orange staining (Supplementary Fig.S1). TEM analysis showed massive mitochondria degradation in HeLa1.2 cells treated with 100 nM STS (Fig.2D). The degradation was confirmed by Western blotting using COX-IV (an inner mitochondrial membrane marker) antibody (Fig.2A). The rapid decrease of cellular content of COX-IV at 3-h and 6-h after STS treatment was consistent with the LC3-I/II conversion and AVO formation. The dissociation of apoptosis and autophagy in HeLa1.2 cells was further confirmed using another pro-apoptotic drug, actinomycin D [20] (supplementary Fig.S2).

### 3.2 Mitochondrial ROS are not essential for STS induced autophagy in HeLa1.2 cells

Given that neither STS nor ActD displays a direct prooxidant effect, HeLa1.2 cells - in which the autophageal signaling pathway can be initiated independently of apoptosis - represent an ideal experimental model for exploring the role of endogenously generated mitochondrial ROS in autophagy.

To determine whether ROS played a role in STS-induced autophagy in HeLa1.2 cells, generation of superoxide, a one-electron reduction product of molecular oxygen, was first examined using DHE assay. The basal level of oxidation of DHE to ethidium was much lower in HeLa1.2 compared to HeLa cells, possibly due to their decreased mitochondrial respiratory rate (Fig.3A). However, these cells did retain the ability to generate superoxide, albeit to a much lower extent. Indeed, both rotenone (ETC complex I inhibitor, 1  $\mu\text{M}/1\text{h}$ ) and antimycin A (ETC complex III inhibitor, 5  $\mu\text{M}/1\text{h}$ ) significantly increased the intracellular superoxide level in HeLa1.2 cells as evidenced by the elevated ethidium fluorescence responses (Fig.3A). We were further anxious to assess whether conditions leading to STS-induced autophagy would be associated with superoxide production. No detectable change in ethidium fluorescence was observed in HeLa1.2 cells incubated with STS (100 nM) for 1–4 h. Moreover, the mean ethidium fluorescence from cells after prolonged (5–6 h) incubations with STS was slightly lower than that from untreated cells (Fig.3B). Assuming that mitochondria are the major source of ROS, this may be attributed to significant degradation of mitochondria following STS treatment (Fig.2A,D). In line with these results, we found that incubation of HeLa1.2 cells with membrane permeable antioxidant enzymes, PEG-SOD (a mammalian superoxide dismutase conjugated with polyethylene glycol, 100 U/mL) and catalase (50 U/mL) decreased the ethidium fluorescence at baseline in control cells (Fig.3A), indicating the intracellular entry of the enzyme. As shown in Fig.2B, PEG-SOD/catalase exerted no effect on STS-induced LC3-I/II conversion in HeLa1.2 cells. Thus, STS-induced autophagy in HeLa1.2 cells progressed – in the absence of concomitantly developing apoptosis – without production of superoxide.

Given that mitochondrial superoxide is rapidly converted to membrane permeable and relatively stable  $\text{H}_2\text{O}_2$  we examined the intracellular concentration of  $\text{H}_2\text{O}_2$  following STS treatment. We employed two independent protocols: i) DCFH-DA assay and ii) specific protein-based  $\text{H}_2\text{O}_2$  sensors that can be expressed in different compartments of cells [16]. Once diffused into cells, DCFH-DA is hydrolyzed by esterases to DCFH that can be oxidized to DCF by a variety of intracellular hydroperoxides. A significant increase of DCF fluorescence was observed in HeLa cells following STS treatment (100nM, 4–6 h). Under the same conditions, this response was not observed in STS treated HeLa1.2 cells (Fig.3C). Further,  $\text{H}_2\text{O}_2$  levels in HeLa and HeLa1.2 cells exposed to STS were monitored using HyPer-probes targeting cytosol (pHyPer-cyto) and mitochondria (pHyPer-dmito). HyPer has two excitation peaks with maxima at 420 and 500 nm, and one emission peak with a maximum at 516 nm. Upon reaction with  $\text{H}_2\text{O}_2$ , the excitation peak at 420 nm decreases proportionally to the increase in the peak at 500 nm [16]. Therefore, the change of intracellular  $\text{H}_2\text{O}_2$  level could be evaluated by calculating the HyPer fluorescence ratio upon excitation by 488 and 405 nm laser. As demonstrated in Fig.4A, exogenously added  $\text{H}_2\text{O}_2$  increased the Ex488/Ex405 ratio in pHyPer-cyto transfected HeLa1.2 cells in a dose dependent manner (1–20  $\mu\text{M}$ ). Treatment of HeLa1.2 cells with 100 nM STS did not cause significant changes in the fluorescence ratio Ex488/Ex405 at either 3-h or 6-h as assessed by flow cytometry (Fig.4B). Time-lapse imaging showed no changes in the fluorescence during the early stages (1–3 h) of STS induced-autophagy (Fig.4C shows representative time-lapse fluorescence images at the indicated time points). However, both control and STS-treated HeLa1.2 cells responded similarly by an increased fluorescence Ex488/Ex405 ratio to exogenous  $\text{H}_2\text{O}_2$  (10  $\mu\text{M}$ ) thus further supporting the notion that no  $\text{H}_2\text{O}_2$  was generated in STS-treated HeLa1.2 cells at the indicated time points (Fig.4B). Similar data were obtained with cells transfected with pHyPer-dmito (Fig.4C, and data not shown). Thus both DCFH-DA protocol and HyPer assay found no STS-induced  $\text{H}_2\text{O}_2$  production in HeLa1.2 cells. On the other hand, we found that ROS alone (rotenone-induced superoxide generation or exogenously added  $\text{H}_2\text{O}_2$ ) is not sufficient to trigger LC3-I/II conversion in HeLa and HeLa1.2 cells (Fig.2C, and supplementary Fig.S3,4).

### 3.3 STS induced autophagy in mtDNA deficient HeLa1.2 cells

To further evaluate the essentiality of mitochondrial ROS for autophagy induction, we generated *mtDNA* deficient  $\rho^{\circ}$  HeLa1.2 cells. The status of cells as *mtDNA*-depleted was verified by examining the expression of *mtDNA*-encoded cytochrome oxidase II protein using RT-PCR and Western blot analysis (data not shown). The lack of functional mitochondria in the  $\rho^{\circ}$  cells was further confirmed using rotenone and antimycin A. The basal level of ethidium fluorescence in  $\rho^{\circ}$  HeLa1.2 cells was much lower compared to control HeLa1.2 cells. Treatment of  $\rho^{\circ}$  HeLa1.2 cells with ETC inhibitors showed no increase in ethidium fluorescence (Fig.3A). In spite of inability of  $\rho^{\circ}$  HeLa1.2 cells to generate ROS, STS induced LC3-I/II conversion comparable to that in HeLa1.2 cells (Fig. 2A). These data further suggest that mitochondrial ROS are not required for autophagy induction.

## 4. Discussion

In recent years, evidence has been accumulating that ROS are involved in the regulation of autophagy signaling [1–3,7]. The obligatory role of ROS in apoptosis and the intertwining of apoptosis and autophagy pathways [8–13], however, obscured the essentiality of ROS as messengers in autophagy. In this study, we dissected the apoptosis and autophagy signaling pathways in HeLa cells by knocking down *cyt c* to assess the engagement of mitochondrial ROS in autophagy without interference by concomitant apoptosis. Counter to the prevailing view, our data suggest that mitochondrial ROS are not necessary to induce autophagy. It is tempting to speculate that collapse of CL asymmetry and appearance of non-oxidized CL on the surface of mitochondria are driving the recognition of damaged organelles for the mitophagial clearance. If the elimination of damaged or unnecessary mitochondria is delayed or inefficient, the inevitable production of ROS leads to the accumulation of oxidized CL – capable of inducing mitochondrial membrane permeabilization. This model of sequential events in damaged cells suggests that ROS production and CL peroxidation act as a switch from mitophagy to apoptosis [12] or necroptosis [21], but these oxidative stress events are not essential for the execution of autophagy.

According to current views - implying the involvement of ROS in autophagy - Atg4, a recently discovered family of cysteine proteases with at least four homologues in mammalian cells [22], is one of the likely redox-sensitive components of autophagial machinery [7]. It has been well documented that activation of Atg4s is required for the process of LC3 to LC3-I conversion [23], which is conjugated to PE by Atg7, and E1-like enzyme, and Atg3, and E2-like enzyme [24]. PE-lipidated LC3 is further deconjugated by Atg4s after completion of autophagosome. As one of the arguments in favor of ROS as essential for the execution of autophagy, Scherz-Shouval *et al* indicated that a highly conserved cysteine residue, in proximity of the catalytic center, may be a target for the redox regulation of HsAtg4A and HsAtg4B [25]. The authors suggested that formation of sulfenic acid or disulfide bond shield the catalytic center. No experimental data, however, were presented either *in vitro* or *in vivo* to explain how ROS were temporally and spatially controlled to ensure that Atg4 remains active [25]. Another pressing issue is how mitochondria avoid oxidative damage, which could trigger apoptosis signaling by releasing pro-apoptotic factors, while generate sufficient amount of  $H_2O_2$  to diffuse through the mitochondrial membrane into reducing cytosolic environment and oxidize Atg4. It is recognized that autophagy/mitophagy exert a protective role in limiting cell death by removing the dysfunctional/injured mitochondria before they release the deleterious contents. In fact, Scherz-Shouval *et al* reported that starvation induced autophagy in the absence of programmed cell death [25]. Therefore, it would be more logical to speculate that ROS are the initial insults that cause mitochondrial injury, rather than serve as essential messengers in the execution of autophagic pathway. The demonstrated protective effects of

antioxidants on autophagy could be attributed to their efficiency in preventing or eliminating the cause of the initial damage.

In the present study, we alleged that STS-induced autophagy in HeLa1.2 cells was not accompanied by superoxide or H<sub>2</sub>O<sub>2</sub> generation. Moreover, STS induced autophagy in *mtDNA* deficient  $\rho^0$  HeLa1.2 cells, is consistent with a previous report [26], in which the ability of mitochondrial ROS generation was completely abolished. The present data indicated that yet to be identified alternative mechanisms – other than mitochondrial ROS – are involved in the Atg4s regulation in STS-treated HeLa1.2 cells. Recently, several potential mechanisms of Atg4 regulation have been reviewed by Chen *et al* [27]. Nair *et al* [28] have demonstrated a role for Atg18 and Atg21 in the protection of Atg8-PE from cleavage by Atg4. In addition, it has been suggested that the substrate of human Atg4B (pro-LC3 or LC3-PE) cannot access the catalytic cysteine residue; prior conformational changes of Atg4B upon binding to LC3 are required for allowing LC3 access to the catalytic site [29–30]. Assuming that ROS are not required for the execution of autophagy, they can be involved in the induction of oxidative damage to critical biomolecules and organelles thus acting as a cause and indirect initiators of autophagic responses. ROS have also been implicated in the autophagy regulation through the activation of Snf1 [31] and of AMPK [32].

In summary, by using *cyt c* deficient HeLa cells, in which the apoptosis and autophagy signaling pathways are separated, we were able to demonstrate that mitochondrial ROS are not necessary for autophagy induction.

#### Highlights

- Dissection of autophagy from apoptosis in cytochrome c deficient HeLa1.2 cells;
- staurosporine-induced autophagy in HeLa1.2 cells was not accompanied by either superoxide or hydroperoxide generation;
- Autophagy was detectable in *mtDNA* deficient  $\rho^0$  HeLa1.2 cells in which reactive oxygen species generation was completely disrupted;
- Counter to the widespread view mitochondrial ROS are not required for the staurosporine-dependent induction of autophagy.

## Supplementary Material

Refer to Web version on PubMed Central for supplementary material.

## Acknowledgments

Supported by NIH NIAID Grant U19-AI068021 and a pilot project grant U19 A8068021 as well as by NIH grants HL70755, HL094488, and NIOSH grant OH008282.

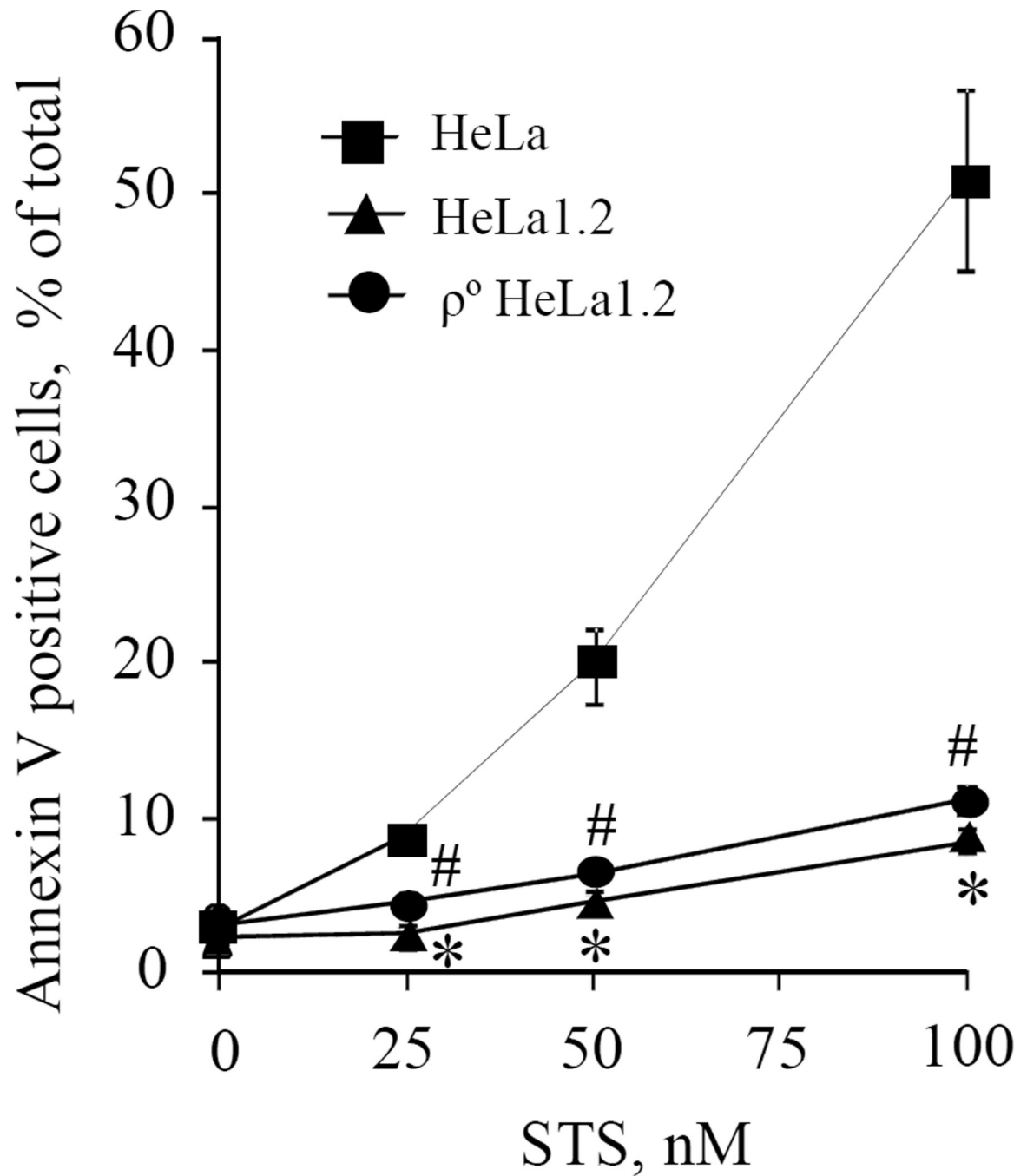
## References

1. Kirkland RA, Adibhatla RM, Hatcher JF, Franklin JL. Loss of cardiolipin and mitochondria during programmed neuronal death: evidence of a role for lipid peroxidation and autophagy. *Neuroscience*. 2002; 115:587–602. [PubMed: 12421624]
2. Botti J, Djavaheri-Mergny M, Pilatte Y, Codogno P. Autophagy signaling and the cogwheels of cancer. *Autophagy*. 2006; 2:67–73. [PubMed: 16874041]

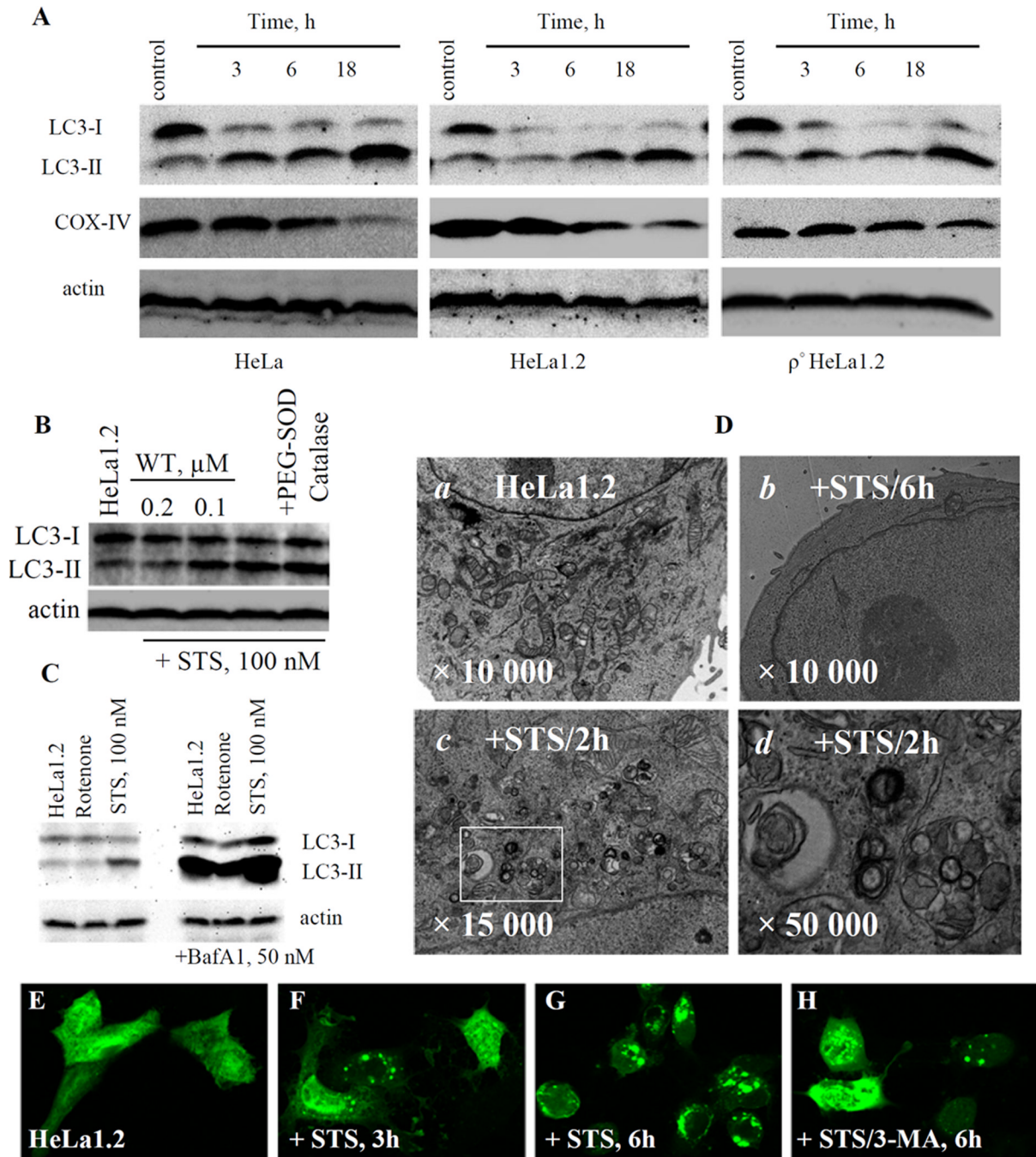
3. Chen Y, McMillan-Ward E, Kong J, Israels SJ, Gibson SB. Mitochondrial electron-transport-chain inhibitors of complexes I and II induce autophagic cell death mediated by reactive oxygen species. *J. Cell Sci.* 2008; 120:4155–4166. [PubMed: 18032788]
4. Baehrecke EH. Autophagy: dual roles in life and death? *Nat. Rev. Mol. Cell Biol.* 2005; 6:505–510. [PubMed: 15928714]
5. Kroemer G, Levine B. Autophagic cell death: the story of a misnomer. *Nat. Rev. Mol. Cell Biol.* 2008; 9:1004–1010. [PubMed: 18971948]
6. Levine B, Sinha S, Kroemer G. Bcl-2 family members: dual regulators of apoptosis and autophagy. *Autophagy.* 2008; 4:600–606. [PubMed: 18497563]
7. Scherz-Shouval R, Elazar Z. ROS, mitochondria and the regulation of autophagy. *Trends Cell Biol.* 2007; 17:422–427. [PubMed: 17804237]
8. Kowaltowski AJ, Castilho RF, Vercesi AE. Opening of the mitochondrial permeability transition pore by uncoupling or inorganic phosphate in the presence of Ca<sup>2+</sup> is dependent on mitochondrial-generated reactive oxygen species. *FEBS Lett.* 1996; 378:150–152. [PubMed: 8549822]
9. Kroemer G, Reed JC. Mitochondrial control of cell death. *Nat. Med.* 2000; 6:513–519. [PubMed: 10802706]
10. Kagan VE, Tyurin VA, Jiang J, Tyurina YY, Ritov VB, Amoscato AA, Osipov AN, Belikova NA, Kapralov AA, Kini V, Vlasova II, Zhao Q, Zou M, Di P, Svistunenko DA, Kurnikov IV, Borisenko GG. Cytochrome c acts as a cardiolipin oxygenase required for release of proapoptotic factors. *Nat. Chem. Biol.* 2005; 1:223–232. [PubMed: 16408039]
11. Petrosillo G, Casanova G, Matera M, Ruggiero FM, Paradies G. Interaction of peroxidized cardiolipin with rat-heart mitochondrial membranes: Induction of permeability transition and cytochrome c release. *FEBS Lett.* 2006; 580:6311–6316. [PubMed: 17083938]
12. Eisenberg-Lerner A, Bialik S, Simon HU, Kimchi A. Life and death partners: apoptosis, autophagy and the cross-talk between them. *Cell Death Differ.* 2009; 16:966–975. [PubMed: 19325568]
13. Fimia GM, Piacentini M. Regulation of autophagy in mammals and its interplay with apoptosis. *Cell Mol. Life Sci.* 2010; 67:1581–1588. [PubMed: 20165902]
14. Li K, Li Y, Shelton JM, Richardson JA, Spencer E, Chen ZJ, Wang X, Williams RS. Cytochrome c deficiency causes embryonic lethality and attenuates stress-induced apoptosis. *Cell.* 2000; 101:389–399. [PubMed: 10830166]
15. Kabeya Y, Mizushima N, Ueno T, Yamamoto A, Kirisako T, Noda T, Kominami E, Ohsumi Y, Yoshimori T. LC3, a mammalian homologue of yeast Apg8p, is localized in autophagosomal membranes after processing. *EMBO J.* 2000; 19:5720–5728. [PubMed: 11060023]
16. Belousov VV, Fradkov AF, Lukyanov KA, Staroverov DB, Shakhbazov KS, Tersikh AV, Lukyanov S. Genetically encoded fluorescent indicator for intracellular hydrogen peroxide. *Nat. Methods.* 2006; 3:281–286. [PubMed: 16554833]
17. Zhu Y, Zhao L, Liu L, Gao P, Tian W, Wang X, Jin H, Xu H, Chen Q. Beclin 1 cleavage by caspase-3 inactivates autophagy and promotes apoptosis. *Protein Cell.* 2010; 1:468–477. [PubMed: 21203962]
18. Christensen ST, Chemnitz J, Straarup EM, Kristiansen K, Wheatley DN, Rasmussen L. Staurosporine-induced cell death in *Tetrahymena thermophila* has mixed characteristics of both apoptotic and autophagic degeneration. *Cell Biol. Int.* 1998; 22:591–598. [PubMed: 10452827]
19. Tafani M, Minchenko DA, Serroni A, Farber JL. Induction of the mitochondrial permeability transition mediates the killing of HeLa cells by staurosporine. *Cancer Res.* 2001; 61:2459–2466. [PubMed: 11289115]
20. Arnould D, Parone P, Martinou JC, Antonsson B, Estaquier J, Ameisen JC. Mitochondrial release of apoptosis-inducing factor occurs downstream of cytochrome c release in response to several proapoptotic stimuli. *J. Cell Biol.* 2002; 159:923–929. [PubMed: 12486111]
21. Vandenabeele P, Galluzzi PL, Vanden Berghe T, Kroemer G. Molecular mechanisms of necroptosis: an ordered cellular explosion. *Nat. Rev. Mol. Cell Biol.* 2010; 11:700–714. [PubMed: 20823910]
22. Mariño G, Uría JA, Puente XS, Quesada V, Bordallo J, López-Otín C. Human autophagins, a family of cysteine proteinases potentially implicated in cell degradation by autophagy. *J. Biol. Chem.* 2003; 278:3671–3678. [PubMed: 12446702]



23. Kirisako T, Ichimura Y, Okada H, Kabeya Y, Mizushima N, Yoshimori T, Ohsumi M, Takao T, Noda T, Ohsumi Y. The reversible modification regulates the membrane-binding state of Apg8/Aut7 essential for autophagy and the cytoplasm to vacuole targeting pathway. *J. Cell Biol.* 2000; 151:263–276. [PubMed: 11038174]
24. Ichimura Y, Kirisako T, Takao T, Satomi Y, Shimonishi Y, Ishihara N, Mizushima N, Tanida I, Kominami E, Ohsumi M, Noda T, Ohsumi Y. A ubiquitin-like system mediates protein lipidation. *Nature.* 2000; 408:488–492. [PubMed: 11100732]
25. Scherz-Shouval R, Shvets E, Fass E, Shorer H, Gil L, Elazar Z. Reactive oxygen species are essential for autophagy and specifically regulate the activity of Atg4. *EMBO J.* 2007; 26:1749–1760. [PubMed: 17347651]
26. Suzuki SW, Onodera J, Ohsumi Y. Starvation induced cell death in autophagy-defective yeast mutants is caused by mitochondria dysfunction. *PLoS One.* 2011; 6:e17412. [PubMed: 21364763]
27. Chen Y, Klionsky DJ. The regulation of autophagy - unanswered questions. *J. Cell Sci.* 2011; 124:161–170. [PubMed: 21187343]
28. Nair U, Cao Y, Xie Z, Klionsky DJ. Roles of the lipid-binding motifs of Atg18 and Atg21 in the cytoplasm to vacuole targeting pathway and autophagy. *J. Biol. Chem.* 2010; 285:11476–11488. [PubMed: 20154084]
29. Noda NN, Ohsumi Y, Inagaki F. ATG systems from the protein structural point of view. *Chem. Rev.* 2009; 109:1587–1598. [PubMed: 19236009]
30. Satoo K, Noda NN, Kumeta H, Fujioka Y, Mizushima N, Ohsumi Y, Inagaki F. The structure of Atg4B-LC3 complex reveals the mechanism of LC3 processing and delipidation during autophagy. *EMBO J.* 2009; 28:1341–1350. [PubMed: 19322194]
31. Kim EH, Sohn S, Kwon HJ, Kim SU, Kim MJ, Lee SJ, Choi KS. Sodium selenite induces superoxide-mediated mitochondrial damage and subsequent autophagic cell death in malignant glioma cells. *Cancer Res.* 2007; 67:6314–6324. [PubMed: 17616690]
32. Hong SP, Carlson M. Regulation of Snf1 protein kinase in response to environmental stress. *J. Biol. Chem.* 2007; 282:16838–16845. [PubMed: 17438333]

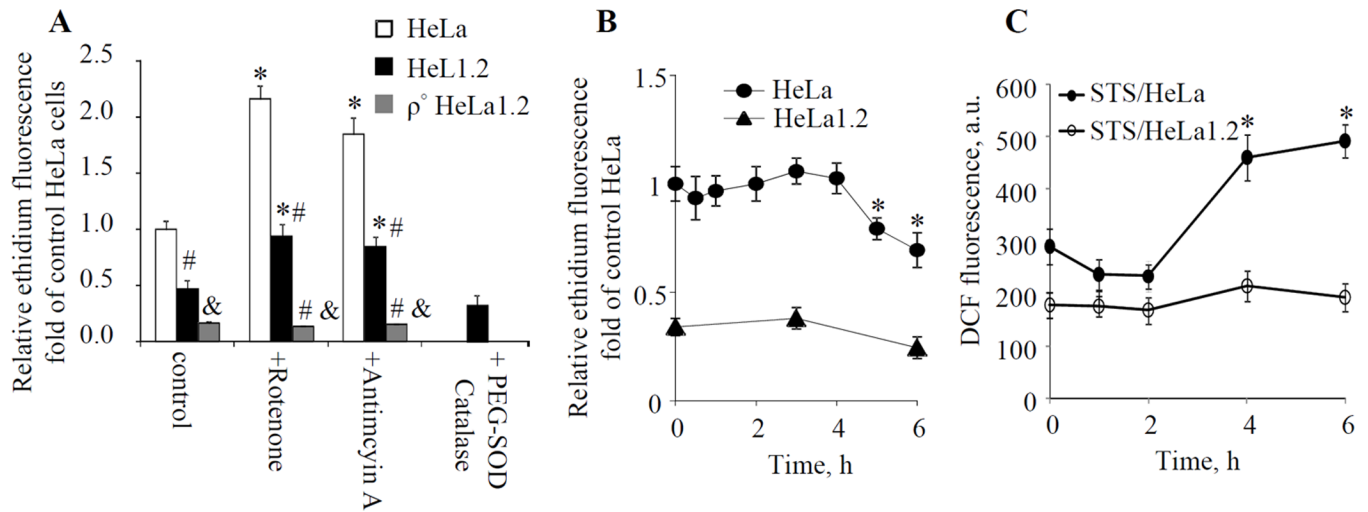


**Fig. 1.**  
 (A) STS-induced apoptosis in HeLa cells, *cyt c* deficient HeLa1.2 cells, and mitochondrial DNA deficient  $\rho^0$  HeLa1.2 cells assessed by PS externalization using flow cytometry. Data presented are mean $\pm$ SD (n=3). #\*  $p < 0.05$  vs HeLa cells under the same condition.

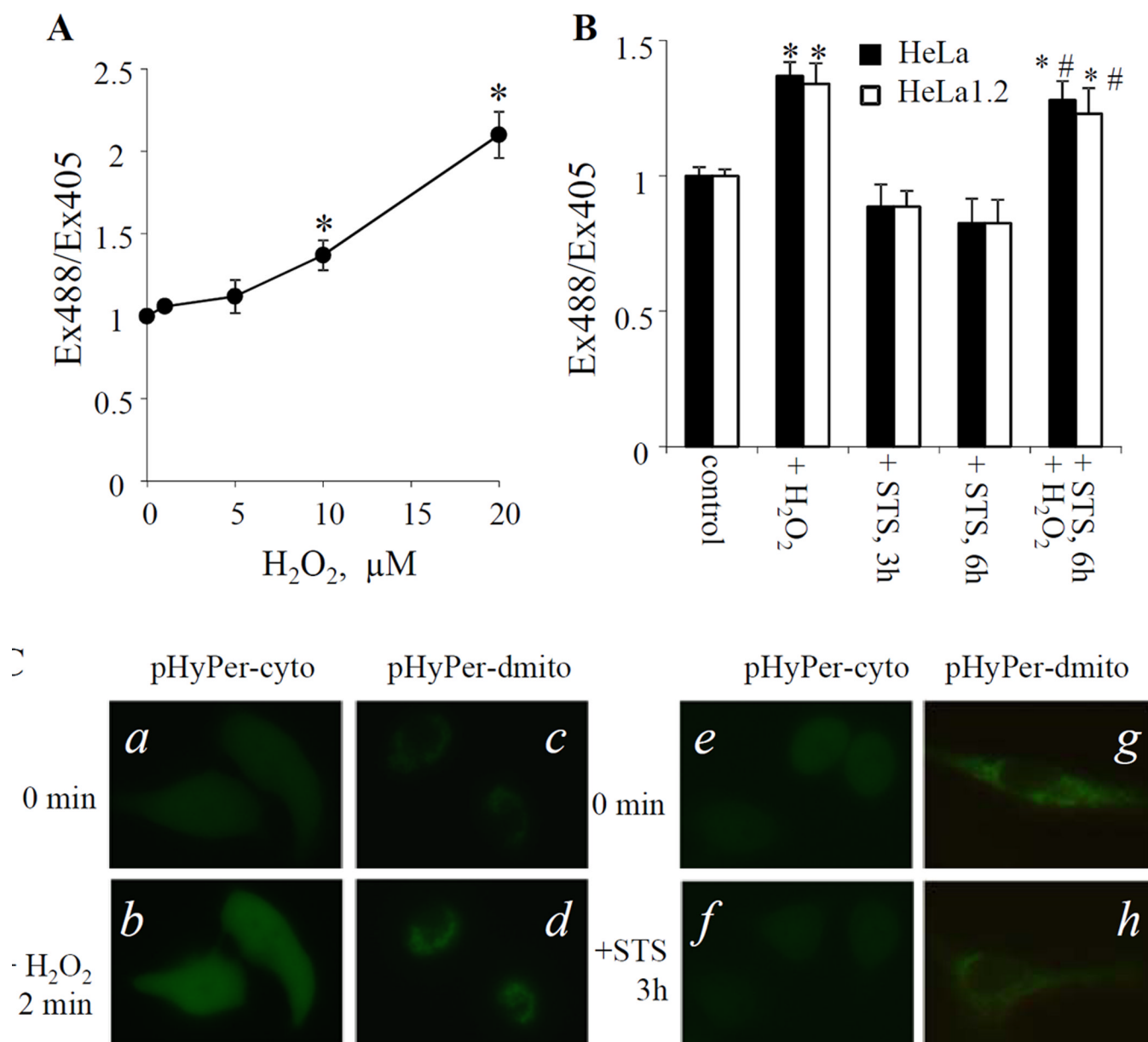


**Fig. 2.**

(A) Western blotting of LC3-I/II conversion and COX-IV degradation in STS-treated HeLa cells, HeLa1.2 cells, and ρ° HeLa1.2 cells. (B) Effect of wortmannin and PEG-SOD on STS-induced LC3-I/II flux in HeLa1.2 cells. (C) Effect of Bafilomycin-A1 on rotenone- and STS-induced LC3-I/II conversion in HeLa1.2 cells. (D) TEM of STS-treated HeLa1.2 cells. (a) control; cells treated with STS for 6h (b) and 2h (c); (d) Enlargement of the rectangular selected area in c. Data presented are representative of three independent experiments. (E–H) Representative confocal images of HeLa1.2 cells transiently expressing GFP-LC3.



**Fig. 3.** (A) Effect of ETC inhibitors (rotenone and antimycin A) and PEG-SOD on superoxide generation in HeLa, HeLa1.2 and ρ<sup>0</sup> HeLa1.2 cells analyzed by DHE assay. (B) Time course of superoxide generation in HeLa and HeLa1.2 cells following STS treatment. (C) Detection of intracellular hydrogen peroxide following STS treatment using DCFH-DA assay. \*  $p < 0.05$  vs control cells without STS treatment. #&  $p < 0.5$  vs HeLa cells under the same condition. Data presented are mean ± SD (n=3).

**Fig. 4.**

Detection of intracellular hydrogen peroxide level using HyPer sensor. (A) Dose dependent response of HyPer-cyto sensor to known amount of H<sub>2</sub>O<sub>2</sub> in HeLa1.2 cells revealed by flow cytometry. (B) Changes of HyPer-cyto fluorescence in STS-treated HeLa and HeLa1.2 cells examined by flow cytometry. (C) Representative time-lapse fluorescence images of HyPer-cyto and HyPer-dmito sensors in H<sub>2</sub>O<sub>2</sub>- (*a-d*, 200 μM, recorded every 30 s for 10 min) or STS- (*e-h*, 100 nM, recorded every 15 min for 3 h) treated HeLa1.2 cells. Data presented are mean±SD (n=3). \* *p* < 0.05 vs untreated control cells, # *p* < 0.05 vs cells treated with STS alone.